chemistry proceedings

MDPI

Proceeding Paper

Fabrication and Characterization of New Er-Doped Yttrium–Scandium–Aluminum–Garnet Ceramics †

Elena Dobretsova [1,*], Vadim Zhmykhov [1], Sergey Kuznetsov [1], Marina Nikova [2], Irina Chikulina [2], Vitaly Tarala [2], Dmitry Vakalov [2], Roman Khmelnitsky [3], Lubov Badyanova [1], Alexandr Pynenkov [4], Konstantin Nishchev [4], Yurii Pyrkov [1], Vladimir Seregin [1] and Vladimir Tsvetkov [1]

1 Department of Laser Crystals, Prokhorov General Physics Institute of the Russian Academy of Sciences, 38 Vavilova Street, 119991 Moscow, Russia; vadimzhmykhov56@gmail.com (V.Z.); kouznetzovsv@gmail.com (S.K.); badyanova.lubov@gmail.com (L.B.); pyrkovyun@lsk.gpi.ru (Y.P.); seregin@lsk.gpi.ru (V.S.); tsvetkov@lsk.gpi.ru (V.T.)
2 Scientific and Laboratory Complex Clean Room, North Caucasus Federal University, 2 Kulakova Prospect, 355028 Stavropol, Russia; m-s-shama@yandex.ru (M.N.); iraaaa@yandex.ru (I.C.); vitaly-tarala@yandex.ru (V.T.); megadims@gmail.com (D.V.)
3 Lebedev Physical Institute, Russian Academy of Sciences, 53 Leninsky Prospect, 119991 Moscow, Russia; khmelnitskyra@lebedev.ru
4 Physics and Chemistry Institute, National Research Mordovia State University, 68 Bolshevistskaya Street, 430005 Saransk, Russia; alekspyn@yandex.ru (A.P.); nishchev@inbox.ru (K.N.)
* Correspondence: eadobr@kapella.gpi.ru
† Presented at the 3rd International Online Conference on Crystals, 15–30 January 2022; Available online: https://iocc_2022.sciforum.net/.

Abstract: We report the fabrication and characterization of yttrium–aluminum–garnet (Er:YAG) and yttrium–scandium–aluminum–garnet (Er:YSAG) ceramics for the implementation of analysis as an active medium for 1500 nm lasing. High erbium content Er:YAG and Er:YSAG ceramics are fabricated from Er:YAG and Er:YSAG powders, respectively. All ceramic samples belong to the garnet-type cubic structure (space group *Ia3d*) without any traceable impure phases. Including Sc^{3+} in the Er:YAG crystal structure leads to improved mechanical characteristics and elastic–plastic properties of the materials. The optical transmittance of ceramics is affected strongly by including Sc^{3+} and increases up to 60% at about 1500 nm.

Keywords: YAG; ceramics; transparency

check for updates

Citation: Dobretsova, E.; Zhmykhov, V.; Kuznetsov, S.; Nikova, M.; Chikulina, I.; Tarala, V.; Vakalov, D.; Khmelnitsky, R.; Badyanova, L.; Pynenkov, A.; et al. Fabrication and Characterization of New Er-Doped Yttrium–Scandium–Aluminum–Garnet Ceramics. *Chem. Proc.* **2022**, *9*, 18. https://doi.org/10.3390/IOCC_2022-12163

Academic Editor: Younes Hanifehpour

Published: 15 January 2022

1. Introduction

The rare-earth-doped yttrium–aluminum–garnet, RE^{3+}:$Y_3Al_5O_{12}$ (RE^{3+}:YAG), is well-known as an active media for high-power lasers [1–3]. Transparent ceramics were initially developed to replace single crystals in cases of disk geometry [4], as well as multilayer and concentration gradient architectures. A number of authors have studied YAG and YSAG ceramics doped by Tm^{3+} [5], Yb^{3+} [6,7], and Er^{3+} [8]. The ceramics obtained show good laser and optical properties, in particular, transparency of up to 83%. We synthesize $(Y_{0.5}Er_{0.5})_3Al_5O_{12}$ (Er^{3+}:YAG) and $(Y_{0.5}Er_{0.5})_3(Al_{0.8}Sc_{0.2})_5O_{12}$ (Er^{3+}:YSAG) ceramics and investigate their microstructures and transmittance depending on the presence of Sc^{3+} ions.

2. Materials and Methods

Precursor powders were synthesized by the reverse precipitation of metal chlorides ($MeCl_3 \cdot 6H_2O$, where *Me* includes Al, Sc, Y, and Er) into a cooled aqueous ammonia solution of 25% through spraying [6,9,10]. The disaggregated oxyhydrate powders were calcined at 1200 °C for 2 h in an oven. Additionally, some of the powder was calcined at 1600 °C. TEOS was used as a sintering addition at the milling powder stage. Then, the ceramic powders were processed by uniaxial pressing, cold isostatic pressing, and sintering in a vacuum

at 1760–1780 °C for 10 h. After vacuum sintering, the samples were processed through lighting annealing and polished on both sides.

The phase composition and unit cell parameters of the ceramic powders were determined with an Empyrean X-ray diffractometer (PANalytical, Almelo, The Netherlands) using *CuKα* radiation (1.5406 Å). The experimental powder diffraction patterns were compared with the XRD pattern of $Y_3Al_5O_{12}$ from the ICSD database (№ 01-072-1853).

The particle size distribution of the oxyhydrate powders was measured with a laser diffraction technique using the Analysette 22 MicroTecPlus laser particle sizer (Fritsch, Markt Einersheim, Germany).

The microstructure of the ceramic surfaces was scanned on an electron microscope EVO 10 (GmbH Zeiss Microscopy, Jena, Germany). The samples were examined at a 20 kV accelerating voltage with a 9 mm working distance in low vacuum operation (EP = 70 Pa); cathode LaB6. Digital images were captured in tiff format with resolution 1024 × 768 px (0.09 nm/px).

Before SEM imaging, the samples of dry particles were placed onto carbon-adhesive tape. The observations of samples were carried out with a beam current on the samples of 370 pA. The images were captured in backscattered electron mode (BSE).

An examination of chemical composition was carried out on detector Smart EDX (AMETEK, Berwyn, PA, USA) with a beam current of 626 pA for analyses and at a 20 kV accelerating voltage with a 9 mm working distance.

The refractive index was determined with the total internal reflection method with the Metricon refractometer for three wavelengths.

The room-temperature transmittance spectra of the Er^{3+}:YAG and Er^{3+}:YSAG ceramics were recorded in the wide range of 250 to 1700 nm on a Shimadzu UV-3101PC spectrophotometer (Shimadzu, Kyoto, Japan) controlled by a desktop computer.

3. Results and Discussion

Characteristics of the Er^{3+}:YSAG ceramic powders are summarized in Table 1. The average grain size was evaluated as d_{50} = 0.88 μm. X-ray diffraction data (Figure 1) point to the presence of Y_2O_3 as an impurity phase after annealing at 1200 °C. To exclude the impurity phase, the samples were annealed at a higher temperature of 1600 °C. X-ray data of the repeatedly annealed powders included picks corresponding to YSAG only and pointed to the compliance of the initial cationic composition with stoichiometric one. Moreover, differences in unit cell parameters of the powders before and after annealing at 1600 °C implied a particular formation of garnets at 1200 °C and full formation at 1600 °C. The average crystallite size d_{XRD} was about 66 nm, and the ceramic powder may be classified as a nanocrystalline one.

Table 1. Characteristics of the Er^{3+}:YSAG ceramic powder obtained with calcinations at 1200 °C and 1600 °C.

Annealing Temperature	Particle Size Distribution, μm			Phase Composition		d_{XRD}, nm	YSAG unit Cell Parameters, *a*, *Å*
	d_{10}	d_{50}	d_{90}	Er:YSAG	Y_2O_3		
1200 °C	0.22	0.88	2.13	99.2%	0.8%	66 ± 2	11.9904(2)
1600 °C	-	-	-	100%	-	>150	11.9958(2)

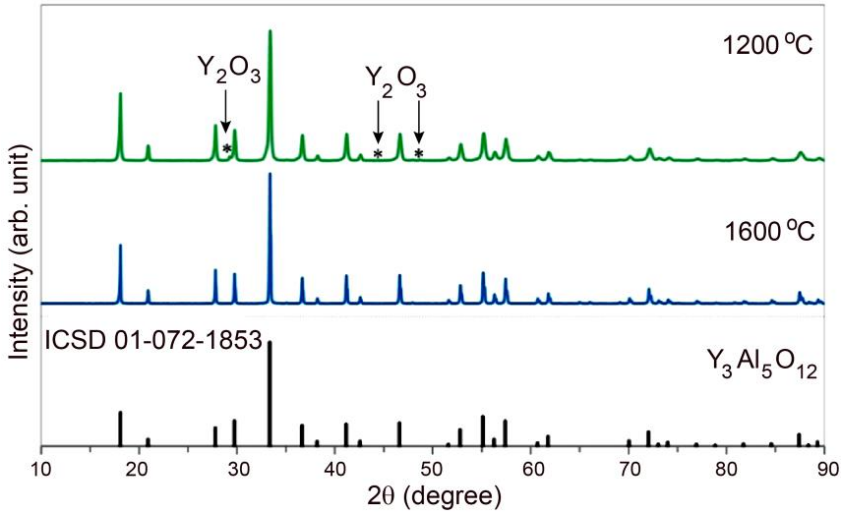

Figure 1. X-ray diffraction pattern of the ceramic powder being calcined at 1200 °C and 1600 °C in comparison with the XRD pattern of $Y_3Al_5O_{12}$ from the ICSD database (№ 01-072-1853).

Experimental data of refractive indices for three wavelengths (Table 2) were subsequently fitted using a least-squares fitting program to the Sellmeier dispersion Equation (Figure 2):

$$\frac{1}{n^2 - 1} = -\frac{A}{\lambda^2} + B \quad (1)$$

where (–A), the slope of the plot of $(n^2 - 1)^{-1}$ versus λ^{-2}, gives a measure of dispersion and B, the intercept of the plot at $\lambda = \infty$, gives $n_\infty = (1 + 1/B)^{1/2}$.

Table 2. Measured refractive indices of the ceramic samples and coefficients in the Sellmeier dispersion equation.

Ceramic Samples	Refractive Indices			Coefficients in the Sellmeier Dispersion Equation	
	633.5 nm	969.0 nm	1539.5 nm	A	B
Er:YAG	1.8386(5)	1.8259(5)	1.8167(5)	$6.9(1.4)\cdot10^3$	$4.36(2)\cdot10^{-1}$
Er:YSAG	1.8487(5)	1.8359(5)	1.8257(5)	$6.9(1.1)\cdot10^3$	$4.30(2)\cdot10^{-1}$

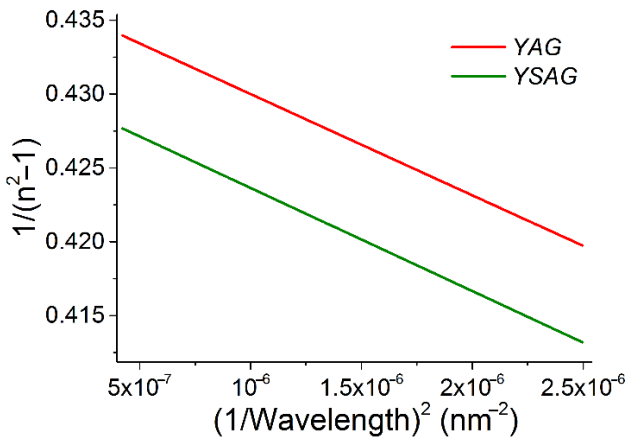

Figure 2. Refractive index (n)–wavelength (λ) dependence.

Figure 3a,b show the SEM micrographs of the Er^{3+}:YAG and Er^{3+}:YSAG ceramics, respectively. Er^{3+}:YAG includes many pores that might be scattering centers. The surfaces of the Er^{3+}:YSAG ceramics demonstrate a homogenious texture, and the number of pores

decreases significantly. Energy-dispersive X-ray spectroscopy (EDX) analysis shows overstated Al^{3+} content in the ceramics, in particular, 5.1(4) and 5.4(5) atoms per formula unit (apfu) in Er:YSAG and Er:YAG, respectively. This is explained by an instrument error up to 10%. Thus, Sc^{3+} can occupy dodecahedral and octahedral structural position and substitute Y^{3+} and Al^{3+}, respectively. The empirical formulas calculated based on twelve oxygen atoms per formula unit are $Er_{1.26}Y_{1.17}Sc_{0.49}Al_{5.08}O_{12}$ and $Er_{1.36}Y_{1.23}Al_{5.41}O_{12}$.

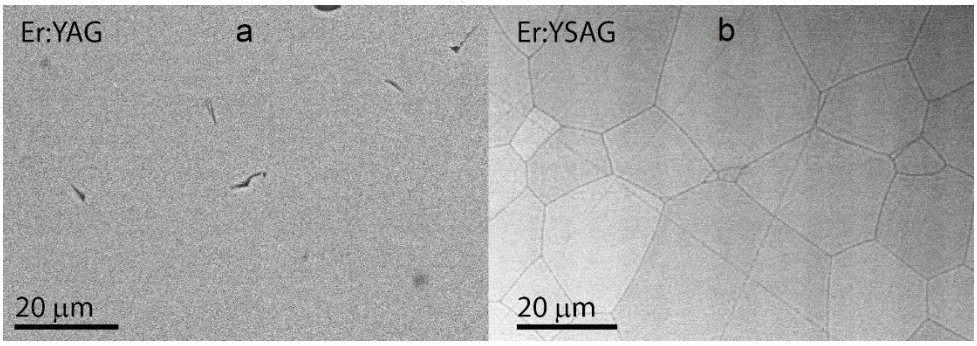

Figure 3. SEM micrographs of the (**a**) Er:YAG and (**b**) Er:YSAG ceramic surfaces.

Probably, the presence of Sc^{3+} in the YAG crystal structure leads to decreasing melting temperature and the improved elastic–plastic properties of the materials. As a result, the Er:YSAG ceramic sample has a more perfect microstructure and higher optical transmittance (Figure 4).

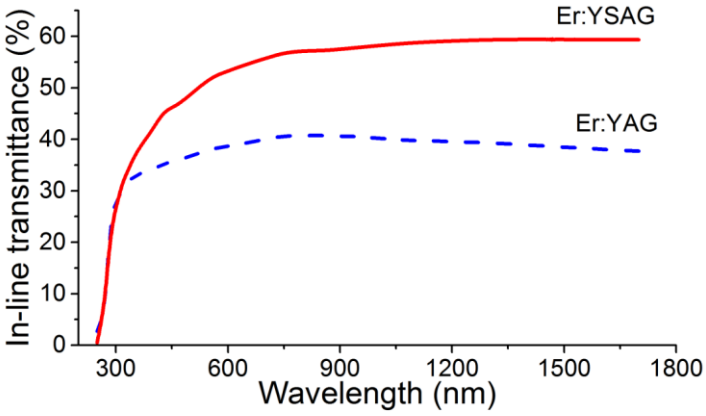

Figure 4. In-line transmittance of the Er^{3+}:YAG (blue) and Er^{3+}:YSAG (red) samples.

Author Contributions: Conceptualization, E.D., S.K. and V.T. (Vladimir Tsvetkov); methodology, S.K., V.T. (Vitaly Tarala) and K.N.; formal analysis, V.Z., I.C., M.N., D.V., R.K., L.B. and A.P.; investigation, E.D., V.Z., I.C., M.N., D.V., R.K., V.T. (Vladimir Tsvetkov), Y.P., V.S. and A.P.; data curation, E.D., D.V., R.K. and A.P.; writing—original draft preparation, E.D. and V.Z.; writing—review and editing, S.K. and V.T. (Vladimir Tsvetkov); visualization, E.D. and V.Z.; supervision, V.T. (Vladimir Tsvetkov). All authors have read and agreed to the published version of the manuscript.

Funding: This research was funded by The Ministry of Science and Higher Education of the Russian Federation, the Grant of the President of the Russian Federation №MK-72.2022.1.2.

Institutional Review Board Statement: Not applicable.

Informed Consent Statement: Not applicable.

Data Availability Statement: Not applicable.

Acknowledgments: The authors acknowledge I Novikov for their assistance in SEM measurements. The ceramic samples have been obtain in Research Equipment Sharing Center of North-Caucasus Federal University.

Conflicts of Interest: The authors declare no conflict of interest.

References

1. Zhang, J.; Schulze, F.; Mak, K.F.; Pervak, V.; Bauer, D.; Sutter, D.; Pronin, O. High-Power, High-Efficiency Tm:YAG and Ho:YAG Thin-Disk Lasers. *Laser Photon. Rev.* **2018**, *12*, 1870018. [CrossRef]
2. Cai, Y.; Xu, B.; Zhang, Y.; Tian, Q.; Xu, X.; Song, Q.; Li, D.; Xu, J.; Buchvarov, I. High power and energy generation in a Nd:YAG single-crystal fiber laser at 1834 nm. *Photon. Res.* **2019**, *7*, 162–166. [CrossRef]
3. Rao, H.; Liu, Z.; Cong, Z.; Huang, Q.; Liu, Y.; Zhang, S.; Zhang, X.; Feng, C.; Wang, Q.; Ge, L.; et al. High power YAG/Nd:YAG/YAG ceramic planar waveguide laser. *Laser Phys. Lett.* **2017**, *14*, 045801. [CrossRef]
4. Lou, Q.; Zhou, J.; Qi, Y.; Cai, Y.Q.A.H. Laser Applications of Transparent Polycrystalline Ceramic. In *Advances in Ceramics-Synthesis and Characterization, Processing and Specific Applications*; IntechOpen: London, UK, 2011; pp. 447–478.
5. Feng, Y.; Toci, G.; Patrizi, B.; Pirri, A.; Hu, Z.; Chen, X.; Wei, J.; Pan, H.; Li, X.; Zhang, X.; et al. Fabrication, microstructure, and optical properties of Tm:Y 3 ScAl 4 O 12 laser ceramics. *J. Am. Ceram. Soc.* **2019**, *103*, 1819–1830. [CrossRef]
6. Nikova, M.; Tarala, V.; Malyavin, F.; Vakalov, D.; Lapin, V.; Kuleshov, D.; Kravtsov, A.; Chikulina, I.; Tarala, L.; Evtushenko, E.; et al. The scandium impact on the sintering of YSAG:Yb ceramics with high optical transmittance. *Ceram. Int.* **2020**, *47*, 1772–1784. [CrossRef]
7. Pirri, A.; Toci, G.; Li, J.; Feng, Y.; Xie, T.; Yang, Z.; Patrizi, B.; Vannini, M. A Comprehensive Characterization of a 10 at.% Yb:YSAG Laser Ceramic Sample. *Materials* **2018**, *11*, 837. [CrossRef] [PubMed]
8. Liu, J.; Liu, Q.; Li, J.; Ivanov, M.; Ba, X.; Yuan, Y.; Lin, L.; Chen, M.; Liu, W.; Kou, H.; et al. Influence of doping concentration on microstructure evolution and sintering kinetics of Er:YAG transparent ceramics. *Opt. Mater.* **2014**, *37*, 706–713. [CrossRef]
9. Dobretsova, E.; Zhmykhov, V.; Kuznetsov, S.; Chikulina, I.; Nikova, M.; Tarala, V.; Vakalov, D.; Khmelnitsky, R.; Pynenkov, A.; Nishchev, K.; et al. The influence of the Sc3+ dopant on the transmittance of (Y, Er)3Al5O12 ceramics. *Dalton Trans.* **2021**, *50*, 14252–14256. [CrossRef] [PubMed]
10. Nikova, M.S.; Tarala, V.A.; Vakalov, D.S.; Kuleshov, D.S.; Kravtsov, A.A.; Kuznetsov, S.V.; Chikulina, I.S.; Malyavin, F.F.; Tarala, L.V.; Evtushenko, E.A.; et al. Temperature-related changes in the structure of YSAG:Yb garnet solid solutions with high Sc concentration. *J. Eur. Ceram. Soc.* **2019**, *39*, 4946–4956. [CrossRef]